Reduction of Precise Point Positioning Convergence Period

Garrett Seepersad and Sunil Bisnath, *York University, Toronto, Canada*

BIOGRAPHY

Garrett Seepersad is a Ph.D. candidate at York University, Toronto, Canada, in the Department of Earth and Space Science and Engineering. He has completed his honours B.Sc. in Geomatics at the University of West Indies and his M.Sc. in Geomatics Engineering at York University. His area of research currently focuses on the development and testing of PPP functional, stochastic and error mitigation models.

Dr. Sunil Bisnath is an Associate Professor in the Department of Earth and Space Science and Engineering at York University in Toronto, Canada. His research interests include geodesy and precise GNSS positioning and navigation.

ABSTRACT

Precise Point Positioning (PPP) has become a popular technique to process GNSS receiver data by applying precise satellite orbit and clock information, along with other minor corrections. Although PPP presents definite advantages such as operational flexibility and cost effectiveness for users, it requires tens of minutes for solution initialization, as carrier-phase ambiguities converge to constant values and the solution reaches its optimal precision.

Pseudorange multipath and noise are the largest remaining unmanaged error sources in PPP. It is proposed that by reducing the effects of multipath and noise on the pseudorange observable, accurate estimates of carrier-phase float ambiguities will be attained sooner, thus reducing the convergence period of PPP. Given this problem, this study seeks to improve management of the pseudorange errors.

The well-known multipath linear combination was used in two distinct ways: 1) to directly correct the raw pseudorange observables, and 2) to stochastically de-weight the pseudorange observables. Corrections to the observables were made in real-time using data from the previous day, and post-processed using data from the same day. The improvements in the solution were calculated with respect to the standard PPP solution, where the raw pseudorange observables were not modified or stochastically de-weighted. Using the post-processed multipath observable has shown improvement in the rate of convergence for 59% of the data, as the pseudorange multipath and noise were effectively mitigated. An improvement in the rate of convergence for 50% of the data was observed when the pseudorange measurements were stochastically de-weighting using the multipath observable. The strength of this model is that it allows for real-time compensation of the effects of the pseudorange multipath and noise in the stochastic model.

INTRODUCTION

PPP has become a popular technique to process data from GPS receivers by introducing precise satellite orbit and clock information. Typically, a dual-frequency GPS receiver is utilized, with the dual-frequency pseudorange and carrier-phase measurements linearly combined to remove the first-order effect of ionospheric refraction. The tropospheric refraction is also estimated along with the position, receiver clock error and real-valued carrier-phase ambiguity parameters from the measurements (Héroux et al., 2004; Kouba et al., 2001; Zumberge et al., 1997).

PPP is considered a cost effective technique as it enables sub-centimetre horizontal and few centimetre vertical positioning with a single GPS receiver; in contrast to methods such as relative GPS, RTK and Network RTK which require multiple receivers. PPP can be used for processing of static and kinematic data, both in real-time and post-processing (Bisnath and Gao 2009; Héroux et al., 2004).

PPP requires a relatively long initialization period (few tens of minutes at least) for the carrier-phase ambiguities to converge to constant values and for the solution to reach its optimal precision. This situation is primarily caused by the estimation of the carrier-phase ambiguities from the relatively noisy pseudoranges. The result is that PPP can take full advantage of the precise but ambiguous carrier-phase observations; however, the length of time it takes to reach the optimal solution is a major disadvantage to the wider use of the technique. If the pseudoranges were more precise then there would be a reduction in the convergence period. Within the PPP community, there has been a lack of attention to mitigate pseudorange multipath and noise. Pseudorange multipath and noise together is the largest remaining unmanaged error source in PPP. This study seeks to address this shortcoming of the technique.

MULTIPATH OBSERVABLE

The coloured noise of the pseudorange consists of the multipath and noise, i.e., multiple signal reflections around the satellite and receiver antenna, in cable connectors, and variations from instrumental delays, and possibly due to temperature variations which can occur at different levels: antenna, cables, amplifiers, splitters, receivers, etc. (Defraigne and Bruyninx, 2007).

To characterize the pseudorange multipath for each satellite, the so-called pseudorange multipath observable is computed (see, e.g., Hofmann-Wellenhof et al., (2001). A linear combination of the measured pseudorange and carrier-phase measurements is used. The carrier-phase multipath and noise, approximately two orders of magnitude smaller than the pseudorange multipath and noise, are neglected. The estimate of pseudorange multipath and noise on L1 is presented in equation 1 and on L2 in equation 2.

$$MP_1 = P_1 - \left(1 + \frac{2}{\alpha - 1}\right) L_1 + \left(\frac{2}{\alpha} - 1\right) L_2 \qquad (1)$$

$$MP_2 = P_2 - \left(\frac{2\alpha}{\alpha - 1}\right) L_1 + \left(\frac{2\alpha}{\alpha} - 1\right) L_2 \qquad (2)$$

where

$$\alpha = \left(\frac{f_1}{f_2}\right)^2$$

f_1: L1 frequency 1.5754 GHz

f_2: L2 frequency 1.2275 GHz

This combination contains primarily pseudorange multipath and noise with no possible distinction between them, plus one constant term associated with phase ambiguities, and one term associated with instrumental delays.

Under the conditions that (1) multipath and noise have a zero-mean during a period Tm, (2) the hardware delays are constant during Tm and (3) no cycle-slips occur during Tm, the multipath and noise can be obtained through equation 3.

$$mp_{L1} = MP_1 - MP_{1T_m} \qquad (3)$$

Where MP_{1Tm} is the average of MP1 over the period Tm. The average is removed in order to remove the constant terms. The quantity mp_{L1} contains the white noise components and multipath components with periods smaller than Tm. These terms will therefore disappear from the observed pseudoranges when correcting them for mp_{L1} (Defraigne and Bruyninx, 2007).

Illustrated in Figure 1 is the multipath for PRN 03 ALGO for DOY 249 of 2011. This site was selected as it showed typical ground bounce multipath which was present at most of the sites processed. The multipath time series for this data has a standard deviation of 28 cm, and illustrates the characteristics of typical ground bounce multipath, as at lower elevations there is higher multipath and as the elevation of the satellite increases, the multipath decreases.

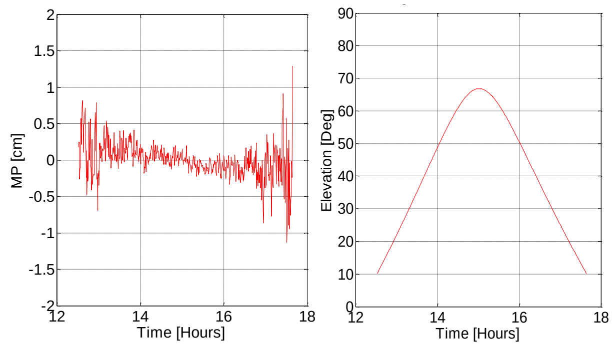

Figure 1: Ionospheric-free pseudorange multipath observable (left) and elevation angle (right) for PRN 03 at Algonquin (ALGO) on DOY 249 of 2011

SATELLITE REPEAT PERIOD

A receiver in static mode, in an unchanged user environment, would have a daily repeatable multipath observable if the so-called sidereal lag is removed and therefore allowing the pseudorange multipath to be corrected for in real-time. Figure 2 illustrates this repeatability of the pseudorange multipath and noise within an offset of approximately 4 minutes. This offset is commonly referred to as sidereal lag, which will be now be explained.

The GPS satellite orbits have a nominal period of one half of one sidereal day (23 h 56 m 4 s) with a daily repeating ground track. Satellite visibility from any point on Earth is the same from day to day, with the satellites appearing in their positions approximately 4 minutes (236 s) earlier each day due to the difference between the sidereal and solar day (Axelrad et al., 2005). The Earth's oblateness has the largest effect on the ground track repeat at the GPS orbit altitude, producing a secular nodal drift westward by ~14.665° per year. To compensate for this motion of the orbit plane, the average semi-major axis of the GPS satellite orbits is set slightly lower, such that the orbital period is about 4 s faster than a sidereal half-day and consequently the time shift of the daily repeat for most satellites in the constellation is closer to 244 s (Axelrad et al., 2005).

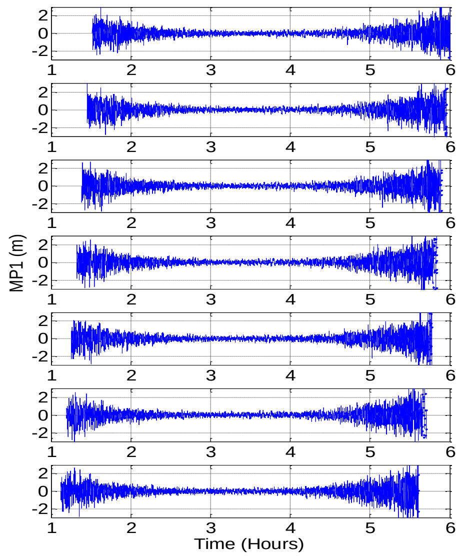

Figure 2: Multipath linear combination for DOY 244-250 for the site ALBH PRN 24 of 2011 showing the daily sidereal lag

There are three methods for estimating the sidereal lag for each GPS satellite geometry: 1) compute the period from the semi-major axis given in the broadcast ephemeris or almanac data; 2) compute the repeat time by interpolating precise orbits to the time of equator crossings; and 3) find the actual repeat geometry for a selected location and identify the associated time shift. Presented in Agnew and Larson (2007) and Axelrad et al. (2005) are analyses of using these three methods to calculate the sidereal lag. Using the broadcast ephemeris and interpolating the precise orbits presented equivalent results. The method using broadcast ephemeris was used here because of its simplistic design and ease of implementation. The sidereal shift (Ta) is computed using the period from the semi-major axis given in the broadcast ephemeris as follows:

$$T_a = 86400 - 2(2\pi/n) \quad (4)$$

Where the mean motion, n, is given by

$$n = \sqrt{\mu_\varepsilon + a^3} + \Delta n \quad (5)$$

and a is the semi-major axis and Δn is the mean motion adjustment. μ_ε is the gravitational constant of the Earth specified as 3.986x$10^{14} m^3/s^2$ for use with the broadcast elements.

IMPLEMENTATION OF PSEUDORANGE MITIGATION USING MULTIPATH OBSERVABLE

The standard PPP software requires dual-frequency measurements to calculate the ionospheric-free pseudorange and carrier-phase observables. Illustrated in Figure 3 is the measurement processing flow present in the standard PPP software augmented with the multipath mitigation module. The module was designed to function under three different modes of operation, this includes 1) the multipath observable generated from the previous day 2) the multipath observable generated from the same day (post-processing) and 3) the multipath observable generated in real-time using a running average (real-time). The multipath observable generated from within the data through post-processing and real-time is correlated. This correlation has not been taken into consideration within the processing. The first step in the module is to obtain the required multipath observable depending on the user defined mode of operation. This is followed by the correction of the raw P1 and P2 measurements by using the respective MP1 and MP2 observables. The final phase is the ionospheric linear combination of the corrected P1 and P2 and the L1 and L2 observables to give P_{IF} and L_{IF} respectively.

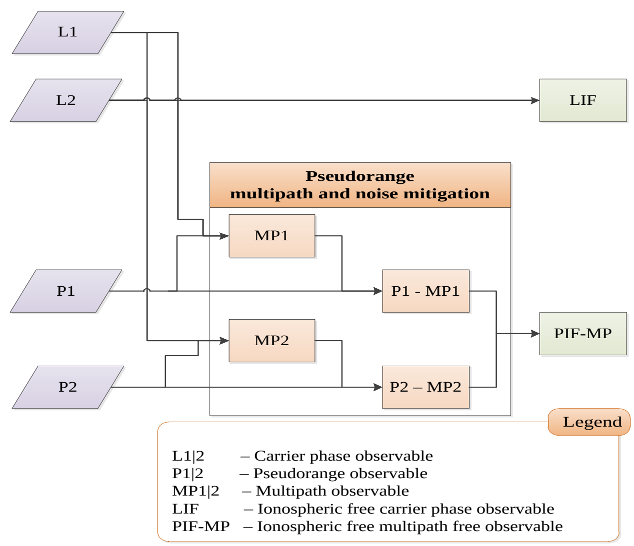

Figure 3: Measurement processing flow augmented by multipath mitigation modules

DATASET AND PROCESSING PARAMETERS

Data from 80 IGS stations observed during DOY 244 to 250 in 2011 were used in the validation of the developed York-PPP software. The sites chosen were a subset of those processed regularly by most IGS ACs, represents a good global distribution. The distribution of the sites is illustrated in Figure 4. Dual-frequency receivers tracking either the C/A or P(Y) pseudorange on L1 were used. Settings used for the evaluation include: the ionospherefree combination of L1 and L2 data, 2 m and 15 mm a priori standard deviations for pseudorange and carrier-phase observations, and 10° elevation cut-off angle.

IGS Final 5 minute orbits, 30 second clocks and Earth rotation parameters products were used. The reference stations are analyzed in static PPP mode. Receiver clocks were estimated epoch-by-epoch. The zenith tropospheric delays were estimated every 60 minutes with an initial STD of 1 m and a power density of 2 cm/sqrt (h). The station coordinates were estimated with an initial constraint of 1 km. The IGS relative antenna model was used and ocean loading and solid Earth tides were obtained from Scherneck (2011) for each of the sites being processed.

Figure 4: Distribution of the selected 80 IGS stations

EXAMINING THE RESULTS OF PSEUDORANGE MULTIPATH AND NOISE CORRECTION

PPP convergence is reliant on the precision of the pseudorange observables. The following methods presented are novel techniques to mitigate pseudorange multipath and noise in PPP. The following section discusses each of the methods applied and quantifies the reduction of the convergence period with the aim of reducing the pseudorange multipath and noise.

To investigate pseudorange multipath and noise for a fixed ground site, the pseudorange multipath observable at site ALGO was analyzed. The results presented in Figure 5 illustrates the multipath observable for PRN 03 on DOY 249 and 250 with the sidereal shift applied. The multipath observable is generated for the data between the elevation angle from 10 to 30° as this time period is most susceptible to ground bounce multipath. Typical ground bounced multipath was observed with a standard deviation of 31.2 cm and 29.8 cm on DOY 249 and 250, respectively. When the multipath observable of both days were subtracted, the standard deviation reduced to 20 cm indicating a reduction in the pseudorange multipath.

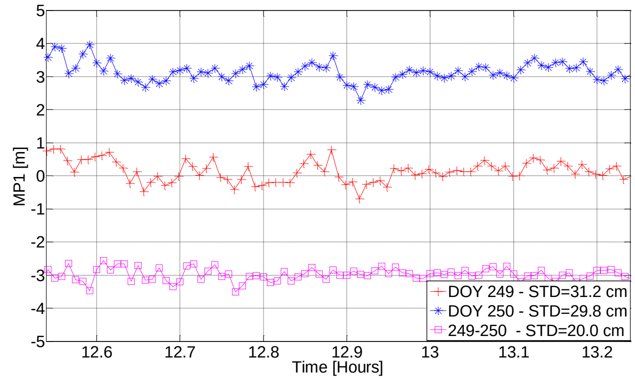

Figure 5: Comparing the pseudorange multipath observable for PRN 03 at ALGO, for DOY 249 and 250 of 2011 in elevation range of 10-30°

Illustrated in Figure 6 is the multipath observable generated from within the dataset. This is only possible through post-processing of the data, as the ambiguity term is eliminated by finding the average of the entire data arc. This method would be the most effective as it accurately represents the pseudorange multipath and noise present within the data. In PPP, the ionospheric linear combination is used, which triples the measurement noise versus the noise on L1 or L2 (Leandro, 2009). This indicates why the multipath observable generated within the same day would highlight a significant reduction in the convergence time of PPP in contrast to the multipath observable from the previous day. In some cases, the noise may not be entirely eliminated as the ambiguity term may not have been accurately removed, as well as biases which may have been introduced.

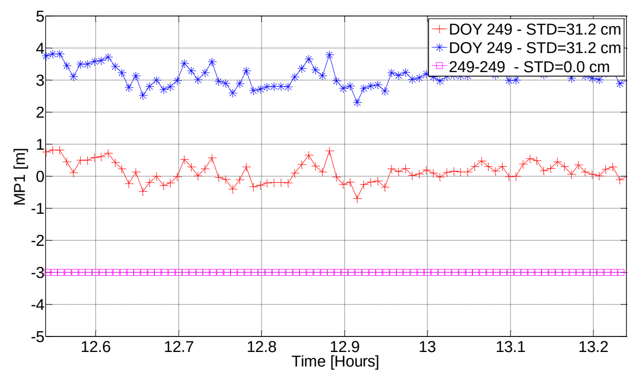

Figure 6: Comparing the pseudorange multipath observable for PRN 03 at ALGO, for DOY 249 of 2011 in elevation range of 10-30°

Illustrated in Figure 7 is another option, this time for real-time pseudorange multipath and noise mitigation. The running average multipath observable recursively estimates the ambiguity as the more data becomes available. The running average is compared to the same day multipath observable. At the site ALGO, the same day multipath observable and the running average had a standard deviation of 31.2 cm and 30.2 cm, respectively, with a difference of 8.1 cm This highlights one of the advantages of using the running average to mitigate pseudorange multipath and noise rather than the multipath observable from the previous day as a static user environment is not required.

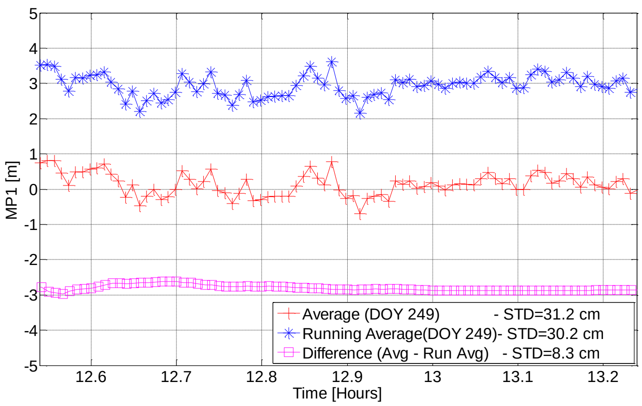

Figure 7: Comparing the pseudorange multipath observable for PRN 03 at ALGO, for DOY 249 of 2011 using running average, in elevation range of 10-30°

The running average is precise, but requires several hours of data to obtain an equivalent level of accuracy as the same day multipath observable. This can be seen in the difference when the average of the entire data arc is removed in contrast to the running-average. The varied running average convergence period is illustrated in Figure 8 and Figure 9. Figure 8 shows how well aligned the real-time and post-processed multipath observable can be. This is due to low multipath and noise during the first few minutes allowing the running average to be properly initialized. There is an initial standard deviation of 10 cm in within the first 10 epochs.

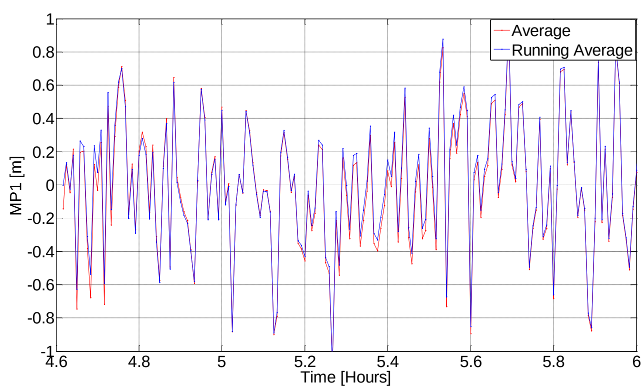

Figure 8: Real-time multipath observable (running-average) with good initialization compared to post-processed multipath observable (average)

Figure 9 illustrates the limitation commonly seen when generating the multipath observable in real-time. The real-time multipath observable illustrates a high level of precision but low accuracy due to the bias present. This is attributed to poor initialization due to a high variation in the pseudorange multipath and noise with a standard deviation of 90 cm within the first 10 epochs.

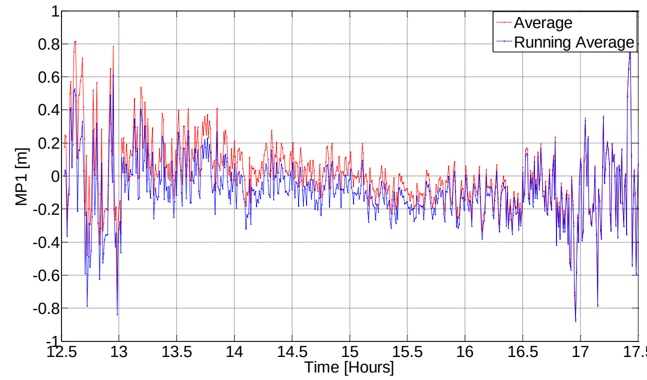

Figure 9: Real-time multipath observable (running-average) with poor initialization compared to post-processed multipath observable (average)

APPLICATION OF TECHNIQUE

Presented in Figure 10 are varying convergence periods at the site FAIR on DOY 245 for scenarios standard PPP, multipath observable used from the previous day, same day and with a running average. A loose convergence threshold of 30 cm was set to examine the time the solution took to converge. The standard PPP solution converged in 2.14 minutes, while the solution using the multipath observable from the previous day or with a running average converged in 2.72 and 4 minutes, respectively. Instantaneous convergence was achieved with the multipath observable from within the same day.

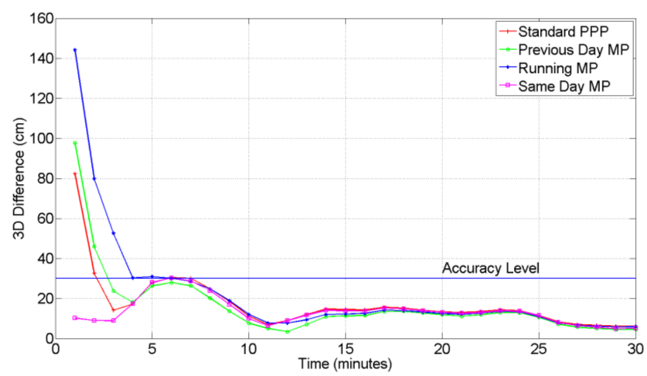

Figure 10: Site FAIR for DOY 245 of 2011, illustrating varying convergence rates based on different pseudorange multipath and noise mitigation techniques

The quality of the residuals for each scenario was examined. Presented in Figure 11 is the precision of the pseudorange residuals for each of the satellites present during initial convergence. The precision of the pseudorange residuals deteriorated for three of eight of the satellites by 7-33%, while improvements in the precision increased by 15-22% for the remaining satellites when the multipath observable from the previous day was applied. Even though this method corrects for the pseudorange multipath, it increases the pseudorange noise. The multipath observable generated from within the same day showed significant improvement ranging from 85-95% and improvements by the running average ranged from 37-76%.

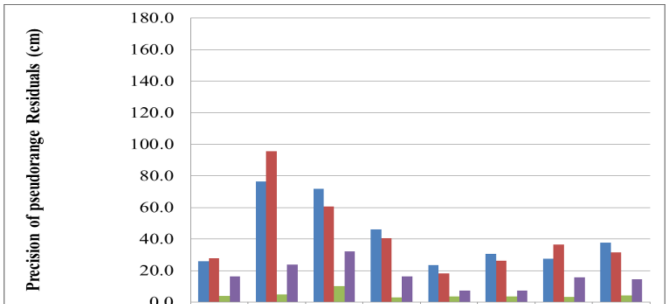

	2	4	10	12	25	29	30	31
Standard PPP	26.1	76.4	71.7	46.0	23.3	30.5	27.4	37.8
Previous Day	27.9	95.7	60.8	40.5	18.1	26.4	36.7	31.7
Same Day	3.9	4.8	10.2	2.9	3.7	3.8	3.4	4.4
Running Average	16.3	23.8	32.2	16.4	7.5	7.3	15.7	14.6

Figure 11: Precision of pseudorange residuals for each satellite for the initial 30 minutes at the site FAIR DOY 245 of 2011

The residuals, shown in Figure 12, were also examined to determine if any biases were introduce and, if so, their magnitude. Using the running average, the biases did not increase for any of the satellites, in contrast to the same and previous day multipath observable where the biases increased for five of the eight satellites present.

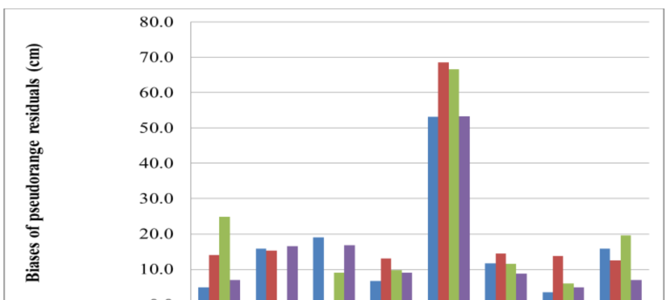

	2	4	10	12	25	29	30	31
Standard PPP	4.9	15.8	19.0	6.6	53.2	11.7	3.5	15.9
Previous Day	14.0	15.2	1.0	13.0	68.6	14.5	13.7	12.5
Same Day	24.8	0.2	9.0	9.8	66.7	11.5	6.0	19.5
Running Average	6.9	16.6	16.8	9.1	53.4	8.7	4.9	6.9

Figure 12: Biases of pseudorange residuals for each satellite for the initial 30 minutes at the site FAIR DOY 245 of 2011

Figure 13 illustrates the distribution of the residuals for PRN 29 for each of the different scenarios. PRN 29 was selected as it showed similar trends for each of the satellites used except for PRN 25, where a significant biases is noted, ranging from 50-70 cm. The distribution of the residuals for the standard PPP and multipath observable from the previous day scenarios were randomly distributed, in contrast to when the same day multipath observable and the running average were applied which in the residuals had a normal distribution.

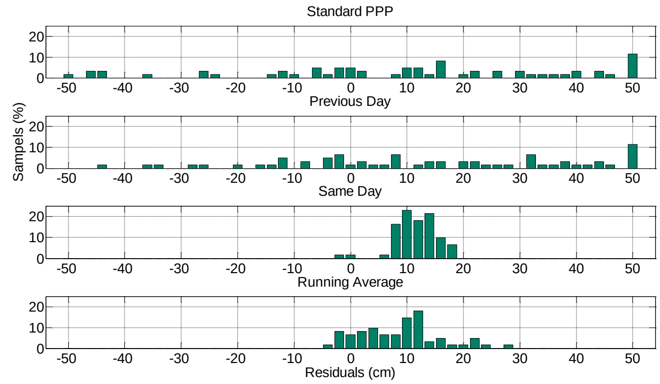

Figure 13: Distribution of pseudorange residuals at site FAIR DOY 245 of 2011 for PRN 29

Similiarly, the same scenarios were examined at the site BAIE (Baie-Comeau, in eastern Canada) for DOY 245 2011. Unlike at the site FAIR, we see a less significant improvement when applying the multipath observable to mitigate the pseudorange multipath and noise effects. Within the first minute, the multipath observable from the previous day reduces the initial solution quality by 4 cm. The running average improves the initial solution by 11 cm. Using the same day multipath observable improves the initial solution by 50 cm. The time the solution takes to the achieve the predefine threshold has been improved by 30 seconds by using the multipath observable from the previous day, while the running average the same day multipath converges to the threshold within a similar time as the standard PPP solution.

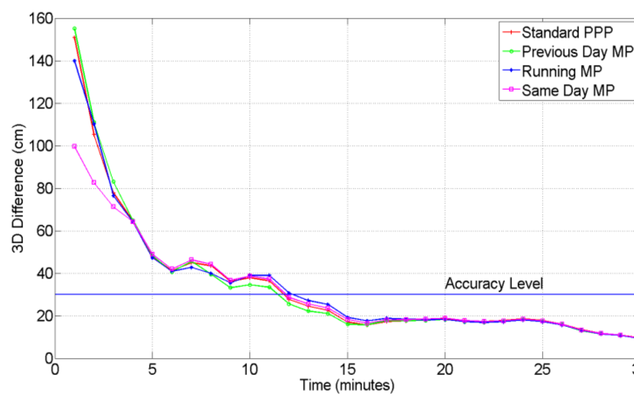

Figure 14: Site BAIE for DOY 245 of 2011, illustrating varying convergence rates based on different pseudorange multipath and noise mitigation techniques

The precision and biases of the residuals are also examined in Figure 15 and Figure 16, respectively. Similar trends to that at FAIR are observed where the scenarios standard PPP and multipath observable from the previous day had similar levels of precision for all satellites present during initialization. The multipath observable generated from the running average and the same day both show significant improvements. The same day multipath observable improved the precision residuals by 50% for PRN 05 and a maximum improvement of 95% was seen for PRN 30. Most improvements ranging from 85-95%. The multipath observable generated using the running average improved the precision by 52% for PRN 02 and as much as 84% for PRN 25. Most of the improvements ranged from 65-85%. To reduced performance of the running average in contrast to the same day multipath observable is observed again, a function of the required convergence time of the observable.

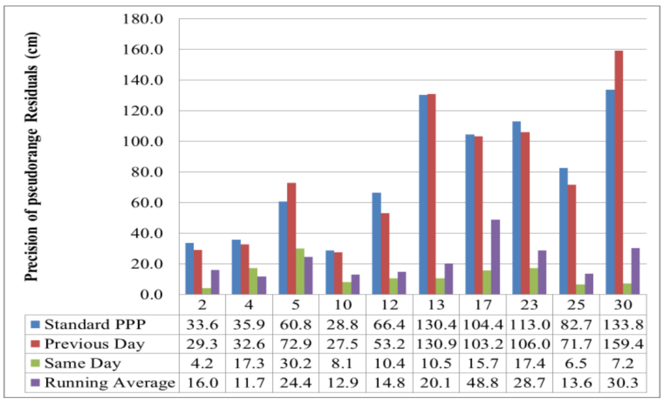

	2	4	5	10	12	13	17	23	25	30
Standard PPP	33.6	35.9	60.8	28.8	66.4	130.4	104.4	113.0	82.7	133.8
Previous Day	29.3	32.6	72.9	27.5	53.2	130.9	103.2	106.0	71.7	159.4
Same Day	4.2	17.3	30.2	8.1	10.4	10.5	15.7	17.4	6.5	7.2
Running Average	16.0	11.7	24.4	12.9	14.8	20.1	48.8	28.7	13.6	30.3

Figure 15: Precision of pseudorange residuals for each satellite for the initial 30 minutes at the site FAIR DOY 245 of 2011

The residuals were also examined in Figure 16 to determine if any biases were introduced and their magnitude. The residuals ranged from 10 to 60 cm for all satellites except PRN 05 with a bias of -167 to -209 cm. Even though PRN 05 illustrated a relatively large bias, it was maintained within the solution, as it did not exceed the current threshold for the pseudorange measurements. The most significant bias introduced by the running average was by 19 cm at PRN 05, while the previous day and same day multipath observables reduced the bias by 23 cm.

Figure 17 illustrates the distribution of the residuals for PRN 02 for each of the different scenarios. PRN 02 was selected as it showed similar trends for each of the satellites used except for PRN 05. The distribution of the residuals for the scenarios standard PPP and the multipath observable from the previous day were randomly distributed. 29% of the residuals were greater than 50 cm for the standard PPP and 11% greater than 50 cm when the previous day multipath observable was used. The same day multipath observable had a normal distribution with a bias of 24.4 cm. The running averaged had a skewed distribution with a mean of 10.6 cm.

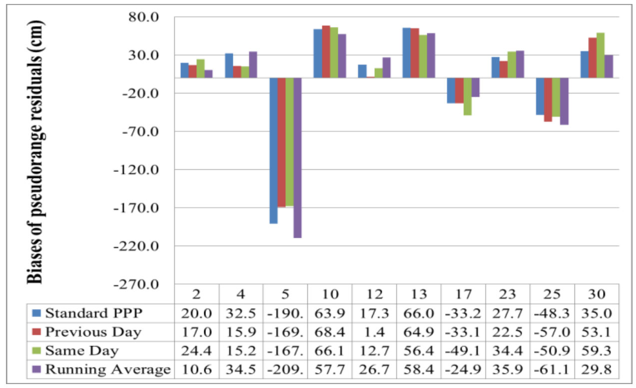

	2	4	5	10	12	13	17	23	25	30
Standard PPP	20.0	32.5	-190.	63.9	17.3	66.0	-33.2	27.7	-48.3	35.0
Previous Day	17.0	15.9	-169.	68.4	1.4	64.9	-33.1	22.5	-57.0	53.1
Same Day	24.4	15.2	-167.	66.1	12.7	56.4	-49.1	34.4	-50.9	59.3
Running Average	10.6	34.5	-209.	57.7	26.7	58.4	-24.9	35.9	-61.1	29.8

Figure 16: Biases of pseudorange residuals for each satellite for the initial 30 minutes at the site FAIR DOY 245 of 2011

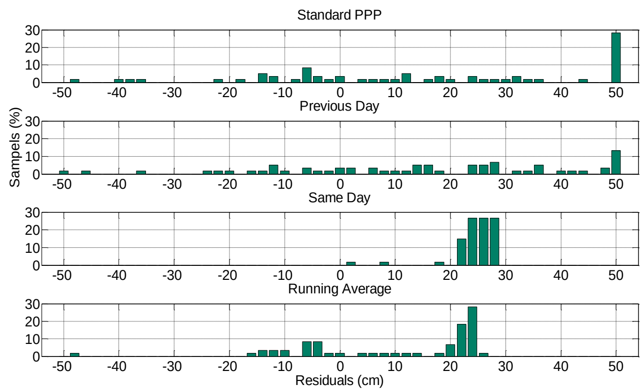

Figure 17: Distribution of pseudorange residuals at site BAIE DOY 245 of 2011 for PRN 29

All 80 sites were processed for each of the scenarios for DOY 245-250 of 2011 with hourly re-initialization for a total of 33 000 datasets. A 30 cm accuracy threshold was set to examine the time the solution took to converge. The results are presented in Figure 18. The most critical time for convergence is within the first 20-30 minutes when the carrier phase measurements are as accurate as the pseudorange measurements. The most significant improvements were noted within the initial 10 minutes which shall serve as the focus of the analysis.

<u>Multipath observable from the previous day</u>: Improvements of 1.3, 2.5, 1.6 and 0.7% were seen in contrast to the standard PPP solution for the 0, 2, 4 and 6 minute time bin. This illustrates that, while improvements were minimal, it is useful to make use of data from the previous day if the information is available. It is important to take note of this methods primary limitation which is a repeated multipath environment is required. A 6% improvement was noted during the initial 10 minutes of convergence in contrast to the standard PPP solution.

Multipath observable from the same day: This method is possible by post-processing the dataset, generating the multipath observable that is fed into the PPP processor. This method has shown significant improvement in the rate of convergence because the real-valued ambiguity term is accurately removed and the multipath observable is generated from the entire dataset, and it accurately represents the pseudorange multipath and noise present. Also, unlike the running average, using the same day multipath observable provides corrections during the first epoch, thus improving the initial coordinate which is critical for reducing convergence period in PPP. Comparing the improvements between applying the multipath observable from the previous day to that generated within the dataset highlights that the noise on the pseudorange observable is one of the primary reasons for the current convergence period within the standard PPP solution. Improvements of 7.2, 14.3, 14.4 and 11.4% were seen in contrast to the standard PPP within the 0, 2, 4 and 6 minute time bin. An improvement in the rate of convergence for 59% of the data was observed within the first 10 minutes.

Multipath observable using a running average: The least effective method was the running average, producing similar results as the standard PPP. This was expected, as both the PPP solution and the running average both have a convergence period due to the required estimation of the ambiguity parameter. The lack of performance of this strategy is attributed to the high quality geodetic receivers used, which record observations with a magnitude of multipath and noise lower than that of the accuracy of the pseudorange observables. Also, similar to PPP, both these methods recursively estimate the ambiguity term present in the carrier phase observation requiring several epochs of data to achieve a steady state.

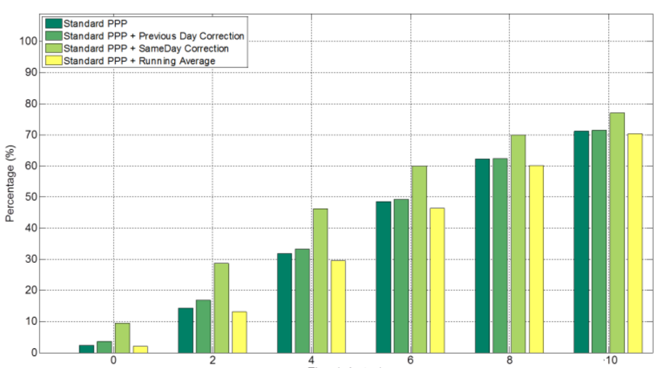

Figure 18: Different pseudorange multipath and noise mitigation techniques to the raw measurements

STOCHASTIC DE-WEIGHTING OF THE PSEUDORANGE MEASUREMENTS USING THE MUTLIPATH OBSERVABLE

The following method has been proposed to take advantage of the precise but biased nature of the running average. Typically, if a stochastic model is used at all, it typically relies on the tracked satellite's elevation angle with respect to the receiver. The use of elevation angle-based weighting is very approximate and its use may produce reduced-accuracy positioning results. The relationships between the observable and other weighting criteria such as the satellite elevation angle are also analyzed. Presented in equation 6 is sigma of unit weight (SUW) used to scale the pseudorange observable which is simple a function of the sine of the elevation angle in radians.

$$SUWPR = sin(ELRAD) \qquad (6)$$

Conceptually, in stochastic de-weighting using the multipath observable, the multipath constituent in the pseudorange functional model is not treated as a deterministic quantity to be estimated, but rather it is coupled with the receiver thermal noise and tracking error terms and its variance is estimated with the linear combination presented in equation 4 and applied to the stochastic model. The strength of this model is it allows for real-time compensation of the effects of the pseudorange multipath and noise in the stochastic model, as long as realistic stochastic models are applied for each epoch in the position estimation process (Bisnath and Langley (2001).

Presented in Figure 19 is the data obtained from ALGO (Algonquin, Canada), DOY 249 for PRN 3. Subplot Figure 19a and Figure 19c illustrates the elevation angle and multipath observable with respect to the time of observation and the respective sigma of unit weight illustrated in Figure 19b and Figure 19d. As expected, the weight derived from the elevation angle of the satellite is a simple weighted function, while the weight derived from the multipath observable does reflects the measurement precision which is a function of the pseudorange multipath and noise.

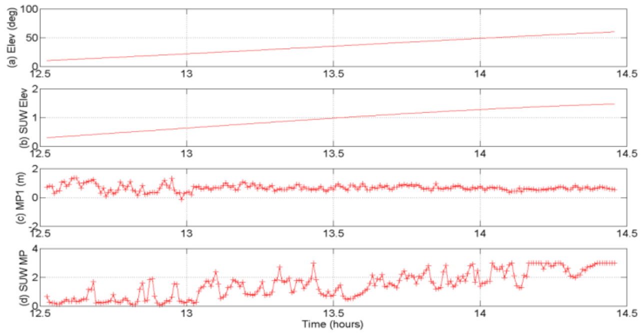

Figure 19: Weighting functions comparison using synthesized P-code observations collected from PRN 3 from ALGO DOY 249 of 2011

Presented in Figure 20 is the stochastic de-weighting used for the pseudorange measurement for PRN 22, DOY 245 from the site BAIE (Baie-Comeau, Canada). One limitations of using the multipath observable is visible at the peak between hours 8-9. It is expected to have maximum weighting as pseudorange multipath and noise is at a minimum, but the satellites are momentarily de-weighted for some epochs.

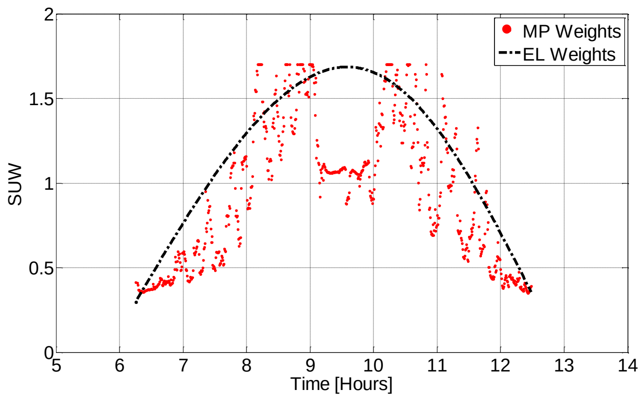

Figure 20: Stochastic de-weighting used for the pseudorange measurement for PRN 22, DOY 245 of 2011 from the site BAIE

At the site FAIR for the DOY 245 the scenarios no weights, elevation weights and multipath weights were examined. Similarly, a 3D accuracy threshold of 30 cm was set, examining the convergence time of the solution, illustrated in Figure 21. The largest convergence period occurred with no weights and elevation weights applied to the pseudorange measurements with a time of 4 minutes. The solution converged the fastest using the multipath weights in a time of 1 minute. When no weights or the elevation weights were applied the initial 3D error was 87 cm; with the multipath weighting scheme applied the 3D error was reduced to 42 cm.

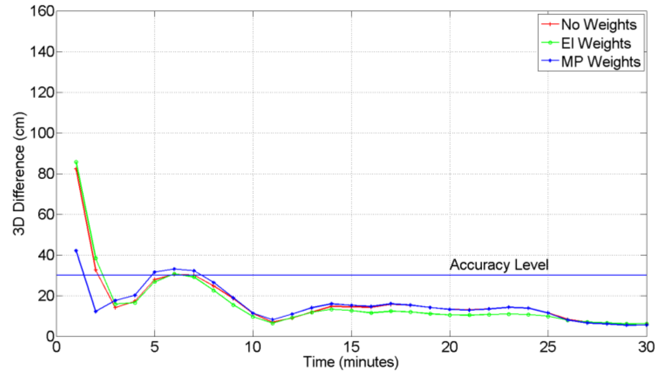

Figure 21: Site FAIR for DOY 245 of 2011, illustrating varying convergence rates based on different pseudorange multipath and noise mitigation techniques

Presented in Figure 22 are varying convergence periods at the site BAIE on DOY 245 for scenarios with no weights, elevation weights and multipath weights. As expected, the largest convergence period occurred with no weights applied to the pseudorange measurements with a time of 13 minutes and elevation weighting had a convergence period of 11 minutes. The solution converged the fastest using the multipath weights in a time of 7 minutes. With no weights applied, the initial solution error was 152 cm. The 3D error was reduced to 129 and 119 cm for the multipath and elevation weights, respectively.

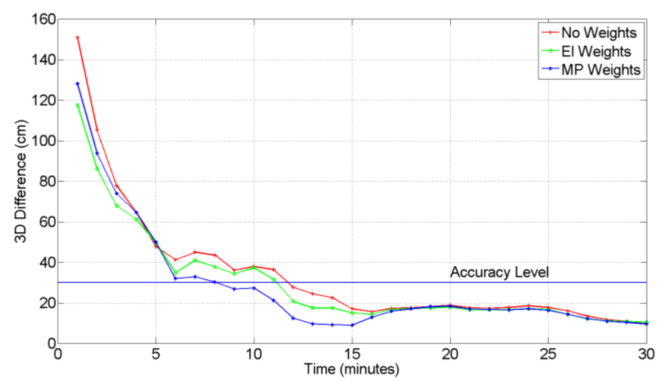

Figure 22: Site BAIE for DOY 245 of 2011, illustrating varying convergence rates based on different pseudorange multipath and noise mitigation techniques

To examine the quality of the improvements on convergence, each stochastic de-weighting method was examined and compared to the standard PPP where the weights are the identity matrix for the pseudorange measurements. This is illustrated in Figure 23. As previously stated, the most critical time period in PPP convergence is the first 30 minutes of data processing. The benefits of either de-weighting method can be easily noted when comparing the standard PPP solution to de-weighting the observations based on either elevation angle or multipath observable. The most influential time period is within the data sets that met the 30 cm 3D threshold within the first 10 minutes. Within the 0, 2, 4 and 6 minute time bins were improvements of 2.2, 11.4, 13.5 and 12%, respectively, when elevation weights were used, and 2.3, 10.7, 12 and 11%, respectively, when the multipath observable weighting scheme was used. The performance of stochastically de-weighting the pseudorange observables using the elevation weights and multipath observable performed comparable.

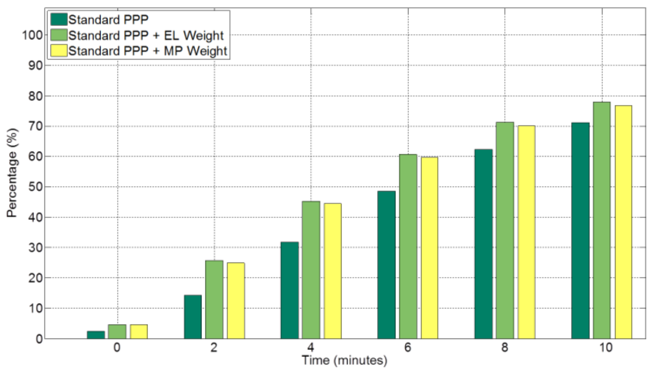

Figure 23: Standard PPP processing parameters with pseudorange observables de-weighted using elevation and multipath weights

CONCLUSION AND RECOMMENDATIONS

If pseudoranges were more precise, there would be a shorter PPP convergence period. Pseudorange multipath and noise are the largest remaining unmanaged error sources in PPP. It is proposed that by reducing the effects of the multipath and noise on the pseudorange observable, carrier-phase ambiguities will reach a steady state at an earlier time, thus reducing the initial convergence and re-convergence period of PPP. The multipath linear combination was calculated to mitigate the raw pseudorange observable based on the magnitude of the pseudorange multipath and noise present. To correct the raw observables three different methods were applied; these included: 1) running average 2) previous day multipath observable, and 3) the same day multipath observable.

The running average filters the pseudorange multipath and noise in real-time. Its major limitation is the requirement of several epochs of data to successfully average the ambiguity term. By using a simple recursive algorithm to estimate the ambiguity term and filter the pseudorange observables may introduce the uncertainty of the ambiguity term present in the running average. After 16 minutes of PPP processing with running average on and off presented equivalent results. Another possible reason why there was a lack of improvements may be attributed to some geodetic receivers that apply a smoothing correction for the pseudorange observables available in the raw data.

Another method analyzed was using the multipath observable from the previous day, where a 6% improvement was noted during the initial 10 minutes of convergence in contrast to the standard PPP solution. Significant improvements were not observed while using this observable, because of the pronounced effect of the pseudorange noise. While improvements were minimal, it is useful to make use of data from the previous day if the information is available, while it is important to take note of this methods primary limitation is a repeated multipath environment is required.

The final method applied to correct the raw pseudorange observable is the use of the multipath observable from within the same day. This method is possible by post-processing the dataset, generating the multipath observable which is fed into the PPP processor. 59% of the data converged faster to meet the 30 cm threshold when the same day filter was used in contrast to the standard PPP solution. This method was most effective as it allowed the ambiguity term to be accurately removed and therefore accurately removed the pseudorange multipath and noise from the pseudorange measurements. Also, unlike the running average, using the same day multipath observable provides corrections during the first epoch, thus improving the initial coordinate, which is critical for reducing convergence period in PPP.

Table 1: Summary of examined methods to mitigate pseudorange multipath and noise by correcting the raw observables

	Raw Pseudorange Correction		
	Previous Day	**Same Day**	**Running Averaging**
Multipath	Yes	Yes	Yes
Noise	No	Yes	Yes
Real-time	Yes	No	Yes
Extra Data Required	Yes	Yes	No
Complexity	High	High	Medium
Limitations	Require data from day before	Post-processing required	Filter has a convergen ce period
% Improved	6%	59%	0%

To utilize the precise but biased nature of the running average a pseudorange multipath and noise stochastic de-weighting scheme was designed. The benefits of either de-weighting using the elevation angle or the multipath observable were observed when compared to the standard PPP solution which used no weights on the pseudorange measurements. A 3D accuracy level of 30 cm was set to examine the improvements of both methods over the standard PPP solution. The most influential time period was observed within the 7 minutes. Overall improvements of 54.5% and 50.5% were observed over standard PPP when using the elevation angle and the multipath observable, respectively.

Table 2: Summary of examined methods to mitigate pseudorange multipath and noise by stochastically de-weighting observables

	Stochastic De-weighting	
	MP Weighting	**El Weighting**
Multipath	Yes	No
Noise	Yes	No
Real-time	Yes	No
Extra Data Required	No	No
Complexity	Medium	Low
Limitations	Tuning required	Too general
% Improved	50.5%	54.5%

Of all the methods presented, the stochastic de-weighting using the running average multipath observable is recommended to become a component of the standard PPP processor. The strength of this model is it allows for real-time compensation of the effects of the pseudorange multipath and noise in the stochastic model, as long as realistic stochastic models are applied for each epoch in the position estimation process. Its performance is comparable to elevation weighting, but with further tuning of the weighting strategy it is expected to show improved performance as was seen for individual sites.

Some of the future work to be done includes further tuning and testing stochastically de-weighting the pseudorange and carrier phase measurements using the running average multipath observable. Also, the integer ambiguity resolution of undifferenced carrier-phase observables has been a difficult task in GPS processing and even more troublesome in PPP, where undifferenced carrier-phase is used. By including the same day multipath linear combination, it is expected to allow the ambiguity to be resolved more efficiently. If the ambiguity term is successfully resolved there will improvements in the convergence period and solution accuracy.

ACKNOWLEDGMENTS

The research reported in this paper was funding from the Natural Sciences and Engineering Research Council of Canada. The results presented in this paper are derived from data and products provided by Natural Resources Canada and the International GNSS Service.

REFERENCES

Agnew, D.C. and K.M. Larson (2007) Finding the repeat times of the GPS constellation, *GPS Solutions*, Vol. 11, No. 1, pp. 71-76.

Bisnath, S. and R. Langley (2001) “Pseudorange multipath mitigation by means of multipath monitoring and de-weighting,” IEEE 4th International Symposium on Kinematic Systems in Geodesy, Geomatics and Navigation, pp. 392–400.

Bisnath, S. and Y. Gao (2009) Current state of precise point positioning and future prospects and limitations, *International Association of Geodesy Symposia*, Vol. 133, pp. 615-623.

Defraigne, P. and C. Bruyninx (2007) On the link between GPS pseudorange noise and day-boundary discontinuities in geodetic time transfer solutions, *GPS Solutions*, Vol. 11, pp. 239-249.

Gao, Y. and K. Chen (2005) Performance Analysis of Precise Point Positioning Using Real-Time Orbit and Clock Products, *Journal of Global Positioning Systems,* Vol. 3, No. 1-2, pp. 95-100.

Héroux, P., Y. Gao, J. Kouba, F. Lahaye, Y. Mireault, P. Collins, K. Macleod, Tetreault, P., and K. Chen (2004) “Products and Applications for Precise Point Positioning - Moving Towards Real-Time,” ION GNSS, Long Beach, CA, pp. 1832 – 1843.

Kouba, J. (2009b) A guide to using International GNSS Service (IGS) Products, http://igscb.jpl.nasa.gov/components /usage.html Accessed: 2012.

Leandro, R.F. (2009) *Precise Point Positioning with GPS: A new approach for Positioning, atmospheric studies and signal analysis*, PhD dissertation, University of New Brunswick, Canada, pp. 1-203.

Seepersad, G. (2012) *Reduction of initial convergence period in GPS PPP data processing*, MSc thesis, York University, Canada, pp. 1-131.

Scherneck, H.-G. (2011) Ocean Tide Loading Provider, http://froste.oso.chalmers.se/loading/index.htm Accessed: 2012.

Zumberge, J.F., M.B. Heflin, D.C. Jefferson, and M.M. Watkins (1997) Precise point positioning for the efficient and robust analysis of GPS data from large networks, *Journal of Geophysical Research*, Vol. 102, No. B3, pp. 5005-5018.